PHYSIOLOGICAL AND PHARMACOLOGICAL CHARACTERIZATION OF THE N1303K MUTANT CFTR

A Thesis

presented to

the Faculty of the Graduate School

at the University of Missouri-Columbia

In Partial Fulfillment

of the Requirements for the Degree

Master of Sciences

---

by

SAMANTHA DESTEFANO

Dr. Tzyh-Chang Hwang, Thesis Supervisor

MAY 2018

The undersigned, appointed by the dean of the Graduate School, have examined the thesis entitled

PHYSIOLOGICAL AND PHARMACOLOGICAL CHARACTERIZATION OF THE N1303K MUTANT CFTR

presented by Samantha DeStefano,

a candidate for the degree of Master of Science,

and hereby certify that, in their opinion, it is worthy of acceptance.

Professor Tzyh-Chang Hwang

Professor Xiaoqin Zou

Professor Luis Polo-Parada

Acknowledgements

I first and foremost thank my primary faculty advisor Dr. Tzyh-Chang Hwang for being so encouraging and supportive as well as challenging me. There is no doubt in my mind that I underestimated how very demanding CF research would be. Even so, Dr. Hwang has been so patient, supportive, kind and complimentary, always finding the positive in what sometimes felt like a sea of failure. I am so humbled and honored to have been given the opportunity to learn from his example of leadership and professionalism. Dr. Hwang's mentorship has been invaluable to me.

Thank you to my thesis committee members, Dr. Xiaoqin Zou and Dr. Luis Polo-Parada for their time and thoughtful review of this thesis body of work. Thank you also to all of the faculty, staff and graduate students of the Department of Medical Pharmacology and Physiology.

Thank you to my lab members Ying-Chun Yu, Wen-Ying Lin, Jingyao Zhang, Jiunn-Tyng Yeh and Han-I Yeh for their helpful discussions and to Shenghui Hu and Cindy Shu for their technical expertise and patience helping me solve technical problems.

I thank Dr. Hao Li of Nanova Biomaterials, Inc. for generous financial support.

Thank you to my family and dear friends, especially my cousin Mike DeStefano who inspires me every day with his courage and grace and was a support when I needed it most.

Table of Contents

List of Figures

Abstract

Background: N1303K, one of the common, severe disease-causing mutations in the *CFTR* gene, causes both defective biogenesis and gating abnormalities of the CFTR protein. The goals of the present study are to quantitatively assess the gating defects associated with the N1303K mutation and its pharmacological response to CFTR modulators including potentiators VX-770 and GLPG1837 and correctors VX-809, and VX-661.

Methods: Gating behavior and pharmacological responses to CFTR potentiators were assessed using the patch-clamp technique in the excised, inside-out mode. We also examined the effects of GLPG1837, VX-770, VX-809 and VX-661 on N1303K-CFTR surface expression using Western blot analysis.

Results: Like wild-type (WT) CFTR, N1303K-CFTR channels were activated by protein kinase A-dependent phosphorylation, but the open probability (P_o) of phosphorylated N1303K-CFTR was extremely low ($\leq$ 0.03 vs ~0.45 in WT channels). In addition, N1303K mutants showed abnormal responses to ATP analogs or mutations that disrupt ATP hydrolysis and/or dimerization of CFTR's two nucleotide-binding domains (NBDs). However, the P_o of N1303K-CFTR was dramatically increased by GLPG1837 (~17-fold) and VX-770 (~8-fold). In addition, VX-809 or VX-661 enhanced N1303K-CFTR maturation by 2 – 3 fold, and co-treatment with GLPG1837 or VX-770 did not show any negative drug-drug interaction.

Conclusion: N1303K has a more severe gating defect than previously reported P_o of ~0.1. Our results suggest a defective function of the NBDs in N1303K-CFTR. An improvement of channel function by GLPG1837 or VX-770 and an increase of Band C protein by VX-809 or VX-661 support a therapeutic strategy of combining CFTR potentiator and corrector for patients carrying the N1303K mutation.

Chapter 1: Introduction

i. CFTR Structure & Gating

The Cystic Fibrosis Transmembrane conductance Regulator (CFTR) is a phosphorylation-activated but ATP-gated anion channel predominantly expressed in epithelial cells [1]. CFTR belongs to the ATP-binding cassette (ABC) superfamily of transporters (ABCC7) and like all other members of the ABC superfamily, CFTR uses the energy of ATP binding and hydrolysis to gate [2]. CFTR is a multi-domain protein made up of two nucleotide-binding domains (NBDs), which are conserved among ABC transporters, two transmembrane domains (TMDs) and a regulatory domain (R-domain), which is unique to this member of the ABC superfamily. This section will provide a general overview of the CFTR structure and then explain how CFTR operates as a chloride channel.

In CFTR, the domains are translated as a single polypeptide chain with two structurally homologous halves each containing a TMD and an NBD [3]. The halves are linked by a regulatory domain (R-domain) which requires phosphorylation by PKA to activate the channel. The newly resolved cryo-EM structure of human CFTR in the closed state showed the R-domain lodged in the middle of the NBDs [4]. Once the R domain has been PKA phosphorylated and moved out of the way to expose the ATP-binding sites on the NBDs, CFTR gating involves ATP binding, NBD dimerization and ATP hydrolysis at the NBDs.

The CFTR NBDs and ATP ligand provide the engine (NBDs) and fuel (ATP) for substrate translocation. Each NBD is divided into an ATP-binding core

subdomain and an α-helical (NBDα) subdomain. The NBDs have six defining motifs: the Walker A, Q-loop, Signature, Walker B, D-loop and H-loop [5]. The core subdomain or “head” subdomain includes the Walker A and B motifs and the switch regions (Q-loop and H-loop). The NBDα subdomain or “tail” contains the ABC Signature and D-loop [3]. The NBDs are arranged in a head-to-tail arrangement which binds two molecules of ATP at two sites with each nucleotide-binding site made up of the head subdomain of one NBD and the tail subdomain of the other NBD. This NBD configuration is in support of the ATP switch model for ABC transporters in which ATP binding and hydrolysis provide a switch inducing conformational changes in the TMDs to open (binding) and close (hydrolysis) the channel.

The TMDs provide the pathway for substrate translocation by CFTR across the cell membrane. Each TMD is made up of six membrane-spanning α-helices (TMs 1-6 in TMD1 and TMs 7-12 in TMD2) connected by alternating extracellular and intracellular helices or “loops” (ECLs 1-4 and ICLs 1-4, respectively). The NBD-TMD coupling interfaces are made up of contacts between NBD1 and ICL4 and NBD2 and ICL2 [6]. ICL1 and ICL3 are in contact with both of the nucleotide binding domains. However, the exact mechanism by which the NBDs are coupled to the gate in the TMDs is still debated [7].

In summary, CFTR’s domains operate as a single unit to drive CFTR gating. One gating cycle of CFTR involves ATP binding, NBD dimerization, ATP hydrolysis and NBD/TMD coupling [8, 9]. ATP binding leads to the formation of an NBD heterodimer which binds two molecules of ATP at two sites. The first site

is a degenerate, non-hydrolytic site. ATP binding site 1 is made up of the head subdomain of NBD1 and the tail subdomain of NBD2. The second site is the consensus site, made up of the head subdomain of NBD2 and the tail subdomain of NBD1. ATP sandwiched at the heterodimer interface leads to channel opening. When the channel opens with both sites occupied by ATP, in the dimerized configuration, this is called ATP-dependent gating. Hydrolysis of the ATP bound at the consensus site (site 2) leads to a partial separation of the dimer and channel closure. When CFTR opens with 1 ATP molecule bound at the nonhydrolytic site, in the partial dimer configuration, this is called ATP-independent gating [10]. This partial dimer lasts tens of seconds and lets another ATP molecule bind to (site 2) NBD2 to initiate a new gating cycle. Cycles of ATP binding and hydrolysis at the NBDs are energetically coupled via the intracellular coupling helices (ICL1-4) to the TMDs to gate the channel.

ii. CFTR Gene Mutations

Cystic Fibrosis (CF) is an autosomal recessive genetic disease caused by mutations in the gene for the Cystic Fibrosis Transmembrane conductance Regulator (CFTR). Over 1900 mutations have been identified [11] and CF pathogenic mutations have traditionally been classified based on their functional defects [12]. Class 1 mutations (ex. W1282X) include nonsense and splice mutations and little to no CFTR protein is made. Class 2 mutations (ex. F508del, N1303K) have defects in protein processing/folding and lead to a reduced quantity of CFTR channels in the plasma membrane. Class 3 and Class 4 mutations have defects in channel gating (Class 3; ex. G551D) or decreased

single channel conductance (Class 4; ex. R117H). Finally, Class 5 mutations result in a reduced amount of normal CFTR protein at the cell surface and Class 6 mutations have reduced cell surface stability.

Some mutations have only one functional defect, while others have multiple defects. In general, mutations in the ATP-binding sites (ex. G1244E, S1251N, G551D, G1349D) have only gating defects. Mutations involved in domain folding or interdomain assembly may have secondary gating defects at the cell surface. For example, F508 has a role in stabilization of the individual NBD1 domain which happens co-translationally. It also has a role in domain assembly. Therefore, F508del has a folding defect, leading to reduced quantity of F508del-CFTR channels reaching the cell surface, gating defects at the cell surface and reduced cell surface stability [13-16]. N1303K is another folding defect mutation with a role in the domain interface and secondary gating defects at the cell surface [17-22]. In general, pore-lining residues in the TMDs have primarily conductance defects, with some exceptions (ex. R347P). Non-pore lining mutations in the TMDs, such as R117H in ECL1, may have conductance and/or gating defects. For mutations with multiple defects, combination therapies targeting each of the mutation's functional defects may be required to restore normal chloride transport activity.

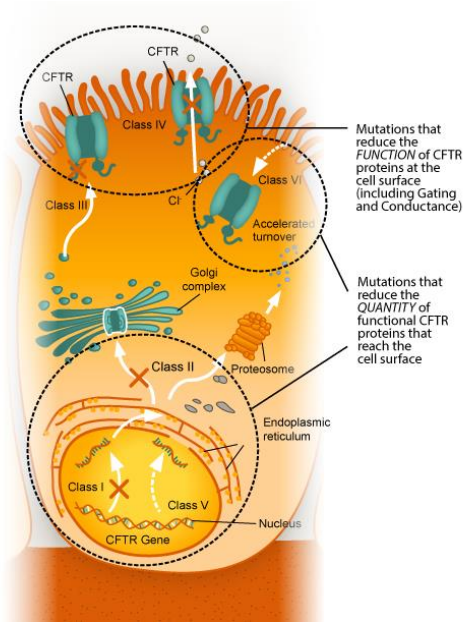

Figure 0-1 Cartoon showing the six classes of CFTR defects [23].

iii. CFTR Pharmacology

CFTR modulators are small molecules designed to target the CFTR mutants' basic underlying cellular defects including transcription, folding, gating and/or cell surface stability. Mutations which exhibit multiple defects, such as F508del and N1303K, require a combination of modulators targeting each of the mutation's functional defects to restore normal chloride transport activity. Correctors target the folding defects and are used to increase the number of channels in the cell membrane. Potentiators target the gating defects and are used to increase channel open probability. This section focuses on the correctors and potentiators used in this study.

CFTR correctors improve CFTR biogenesis, leading to an increase in the amount of CFTR protein that reaches the cell surface. There are three classes of CFTR correctors [24]. Class 3 correctors act on co-translational folding and

stabilize NBD1 energetics. Class 2 correctors stabilize NBD2. Class 1 correctors act on interdomain assembly and are useful for mutations in the domain interfaces. One example of a Class 1 corrector is VX-809 (Lumacaftor). VX-809 acts on the NBD1-CL1/CL4 interface, a region including the F508del disease mutation [24, 25]. Not surprisingly, VX-809 increases the surface pool of F508del-CFTR to about a third of WT-CFTR [26]. VX-661 (Tezacaftor) is an alternative to lumacaftor, with advantageous pharmacologic properties [27]. While CFTR correctors increase the surface pool of CFTR protein, they do not improve the channel's gating properties at the cell surface.

CFTR potentiators increase channel open probability (P_O) at the cell surface. VX-770 (Ivacaftor) was the first identified CFTR potentiator and potentiates several disease-associated gating defect mutations and F508del [15, 28-31]. VX-770 completely rectifies the gating defects of temperature- or pharmacologically-corrected F508del [15]. In the case of F508del, VX-770 increases the P_O of F508del-CFTR mainly by increasing the opening-rate with a smaller increase in the open time [15]. GLPG1837 is a new, highly efficacious but less potent potentiator of CFTR than VX-770 [32]. GLPG1837 acts similarly to VX-770 as a CFTR potentiator and the compounds may share a common binding site. Yeh et al. (2017) discovered that by decreasing the P_O of wild-type channels they decreased the potency but increased the efficacy of GLPG1837 potentiator. The decrease in potency implies state-dependent binding of these compounds.

Although the folding and gating defects of F508del and its pharmacological response to CFTR modulators has been studied extensively, a

quantitative analysis of the gating defects associated with the N1303K mutation is lacking in the literature. In addition, detailed *ex vivo* experiments establishing correctors VX-809 and VX-661 and potentiators VX-770 and GLPG1837 have an effect on the N1303K mutation have not been published.

iv. The NBD-TMD Interfaces

The domain interfaces play an important role in CFTR gating because they relay signals from the cytosolic NBDs, via the intracellular coupling helices (ICL1-4), to trigger conformational changes in the TMDs to open and close the gate [33, 34]. The domain interfaces have the “domain swapping” architecture typical of ABC transporters, wherein each TMD interacts with the NBD in the opposite half of the molecule. The NBD-TMD coupling interfaces are made up of contacts between NBD1 and ICL4 and NBD2 and ICL2 [6]. ICL1 and ICL3 loosely contact both of the nucleotide binding domains. To transmit signals, the TMD must move synchronously with the NBD to which it is connected. The structural basis supporting this signal transmission is depicted as a ball and socket arrangement. Many pathogenic mutations are in the NBD-TMD interfaces, highlighting the importance of these junctures. Pathogenic mutations are unevenly distributed across the two interfaces, with the majority, including the most common CF mutation F508del, targeting the NBD1-TMD interface. Importantly, NBD1 is missing a helix that is present in NBD2 leading to a weaker contact of NBD1 with the TMD compared to NBD2 and making the NBD1/TMD interface more vulnerable to mutation. Interestingly, mutations affecting the coupling interfaces have differential effects on channel gating. Exploring the

details of this structural and functional asymmetry may provide insight into the molecular workings of the transmission interfaces.

The NBD1-TMD interface is made up of residues on the NBD1 surface where IH4 docks and residues in IH4 or near IH4 in the TMD [4, 35, 36]. F508 is one of these such residues in CFTR's nucleotide binding domain 1 which has direct contacts in ICL4. F508 is exposed at the NBD1 surface (Fig. S1 B) in a region comprising the socket component in which the ICL4 (ball component) fits. F508 contributes to an aromatic cluster made up of residues in ICL4 (F1068) and near ICL4 in the TM11 (Y1073, F1074). Close spatial proximity of residue F508 with Y1068 and R1070 provides evidence for π electron interactions with these residues (Fig. S1B). The importance of the structural integrity of this critical interface to channel gating is exemplified in the case of the pathogenic F508del mutation (deletion of the phenylalanine at residue 508). The F508del mutant channel has a single channel open probability (P_O) about 15-fold less than WT-CFTR, due to a lower rate of pore opening [14, 15, 37]. F508del is ATP-responsive [15, 37, 38] and its gating can be improved maneuvers that promote NBD dimerization [15, 37] or abolish ATP hydrolysis [38], albeit with shortened locked-open time and faster ligand-exchange time at ATP-binding site 1. These observations led to the proposal F508del destabilizes the dimeric state of the nucleotide binding domains in CFTR [38]. Alternatively, ATP-binding induced dimerization of the NBDs in F508del may be only loosely coupled to the opening of the gate in the TMDs, resulting in ATP being used less efficiently by the F508del mutant channel. One reason for F508del low efficiency may be because

NBD1 is missing an α helix (h2) (magenta) that is present in NBD2, which may act as a safeguard protecting the NBD-TMD interface from loosening up in NBD2 but not in NBD1.

In contrast to F508, N1303 is buried within the interior of CFTR's second nucleotide binding domain (NBD2), and may have an indirect role in the NBD2-TMD interface. Specifically, N1303 forms a network of hydrogen bonds with a conserved region of the NBD2 called the Q-loop (Q1291). The Q-loop connects the alpha helical subdomain containing the ABC signature sequence to the catalytic core subdomain. Residues in the Q-loop (F1294, F1296) also form part of an aromatic cluster connecting NBD2 to TMD1 via ICL2 (W277). Additionally, the side chain 1303 may be in closer contact with the peptide backbone of Q-loop residue 1296 in the closed, ATP-free state (PDB: 5UAR) than in the open, ATP-bound (PDB: 5W81) state in zebrafish CFTR. This interaction might provide evidence for N1303's role in an intra-NBD2 domain conformational change when ATP binds (site 2).

The N1303K mutation has gating defects that are very different from F508del. While the low P_O of F508del is due mainly to decreased opening rate, N1303K channel has a decreased opening rate and prolonged open time (i.e. decreased closing rate) [20]. Additionally, N1303K prevented pyrophosphate (PPi)-dependent stimulation of current and eliminated ADP-dependent current inhibition [20]. Interestingly, mutation of the conserved Q-loop glutamine (Q1291A) dramatically reduced PPi stimulation, suggesting an interaction of the conserved NBD2 Gln with the bound pyrophosphate is critical either to stabilizing

the bound pyrophosphate or transducing the signal generated by its binding [20]. These data may support the idea of a role for N1303 in an intradomain conformation change, enabling dimerization via interactions of Q1291 with bound nucleotide at site 2.

v. Role of the Q loop in ATP binding

The Q-loop is a conserved region of the NBD which connects the alpha helical subdomain containing the ABC signature sequence to the catalytic core subdomain. It has an important role in coupling bound nucleotide to movement of the alpha-helical subdomain. In this section, the role of the Q loop upon ATP binding will be discussed.

In CFTR and other ABC transporters, ATP binding drives NBD dimerization. The NBDs are relatively flexible in the absence of ATP but ATP binding induces a rigid body rotation of the head and tail subdomains with respect to one another [39-42]. This conformational change is reliant on at least two key interactions: interactions of the γ-phosphate of ATP with the conserved glutamine in the ABC signature motif of the other NBD, and the interaction of the conserved glutamine in the Q loop with bound nucleotide and the hydrolytic water [42]. This conformational change within the NBD aligns residues in the ABC signature motif of one NBD with the Walker A and B motifs of the other NBD, enabling dimerization.

Chapter II: Physiological and Pharmacological Characterization of the N1303K Mutant CFTR

i. Introduction

Cystic Fibrosis (CF) is an autosomal recessive genetic disease caused by mutations in the gene for the Cystic Fibrosis Transmembrane conductance Regulator (CFTR), a phosphorylation-activated but ATP-gated anion channel predominantly expressed in epithelial cells [43]. CFTR regulates the balance of salt and water across epithelial cells lining the exocrine glands, such as the submucosal glands in the lungs, the pancreatic ducts and the sweat glands [44]. N1303K (asparagine-to-lysine mutation at position 1303) is a common, severe CF disease-causing mutation in the CFTR gene (Cystic Fibrosis Foundation Patient Registry 2016 Annual Data Report). As the newly resolved human CFTR structure has shown [4], N1303 is at the equivalent position, but in the opposite half of the CFTR molecule, as F508, deletion of which (F508del) constitutes the most common pathogenic mutation in CF. Like F508del, N1303K is a Class II folding defect mutation, which results in a reduced number of N1303K channels in the cell membrane [17-19]. Both of these common, Class II folding defect mutations also show gating defects once they reach the cell membrane [20-22, 37]. For mutations with both trafficking and gating defects, one therapeutic strategy is to use a combination of CFTR correctors (e.g., VX-809 or Lumacaftor, [26] that increase the number of channels in the cell membrane and CFTR

potentiators (e.g., VX-770 or Ivacaftor, [28]) that enhance the activity or open probability (P_o) of the CFTR channel.

Although the FDA has approved of using Orkambi (Lumacaftor plus Ivacaftor) for the treatment of patients homozygotic for the F508del mutation [45], the clinical benefits are somehow limited partly due to the undesirable drug-drug interaction: Chronic application of Ivacaftor dampens the effects of Lumacaftor [46, 47]. While clinical trials for use of ivacaftor in combination with other first- and next-generation correctors for F508del heterozygotes bearing a minimal function mutation (e.g. N1303K) on their second allele are ongoing, *in vitro* results establishing effects of potentiator VX-770 on the N1303K mutation have not been published. In addition, prior to the discovery of modern day CFTR potentiators, functional studies of CFTR mutants may have underestimated the severity of gating defects associated with these mutations (see ref. [48] for example). Thus, although Berger et. al (2002) showed a P_O of ~0.1 for N1303K [20], this should be considered as a maximal value before more thorough studies are possible.

Recent development of new CFTR potentiators provides powerful tools that afford more accurate assessment of the gating abnormalities caused by CFTR mutations. For example, Yeh et al. (2017) showed that the potentiator GLPG1837 is ~3-fold more efficacious than VX-770 (ivacaftor) on G551D-CFTR [32], the third most common pathogenic mutation with distinct gating defects [49]. Interestingly, the same report also provided evidence that GLPG1837 and VX-770 share a similar mechanism of action perhaps by binding to the same binding

site. Despite its lower potency than VX-770, the high efficacy of GLPG1837, if also true for the N1303K mutation, should make this compound particularly valuable for a more accurate quantification of the gating defect associated with N1303K-CFTR.

In this present study, we used the CFTR potentiators as tools to estimate a maximal P_O of ~0.03 for N1303K. This gating defect likely is caused by dysfunction of CFTR's NBDs as N1303K-CFTR responds to ATP and ATP analogs very differently from WT channels. However, CFTR potentiators such as GLPG1837 and VX-770 dramatically improved the gating function of N1303K-CFTR, suggesting a clinical usefulness of these reagents. Furthermore, we showed that the surface expression of N1303K-CFTR can be enhanced by CFTR correctors VX-809 or VX-661. Unlike the F508del mutation, combination of CFTR potentiators VX-770 or GLPG1837 with VX-809 or VX-661 did not negate the effects of CFTR correctors. Therapeutic strategy of combining CFTR potentiator and corrector for patients carrying the N1303K mutation, and the potential structural mechanism for the gating defects caused by the mutation will be discussed.

ii. Materials and Methods

Cell culture and transfection

Chinese hamster ovary (CHO) cells were grown in 5% CO_2 at 37°C in Dulbecco's modified Eagle's medium supplemented with 10% fetal bovine serum. The cDNA

construct of N1303K-CFTR was co-transfected with pEGFP-C3 (Clontech Laboratories, Inc.) encoding the green fluorescence protein using PolyFect transfection reagent (QIAGEN) according to the manufacturer's instructions. The transfected CHO cells were plated on sterile glass chips in 35-mm tissue culture dishes and incubated at 27°C before patch-clamp experiments.

Western Blot Analysis

CHO cells, in 35mm dishes, were transfected with various DNA construct using X-tremeGENE (Roche). Six hours after transfection, drugs were added to the medium to desired concentrations. Cells were lysed 18 hours post drug treatment using 1xSDS loading buffer. Cell lysates were sheared by pushed through 18G needles. Whole cell lysate were separated in 4~20% gradient gels (Bio-Rad Laboratories) and transferred onto nitrocellulose membranes. The membranes were blocked with 5% milk in TBST buffer (20mM Tris, 137mM NaCl, 0.1% Tween 20) at 4°C overnight. The membranes were then probed with anti CFTR antibody (AB596 from CFTR foundation) and anti-Vimentin antibody (Santa Cruz Biotechnology) at room temperature for two hours. The membranes were washed with TBST five times and then incubated with anti-mouse IgG, HRP linked antibody (Cell Signaling Technology) at room temperature for one hour. The membranes were washed three times with TBST and developed with chemiluminescence reagent (Thermo Scientific). The luminescence was detected by a Molecular Image Chemi Doc (Bio-Rad Laboratories).

Electrophysiological experiments

Details of patch-clamp experiments were described in our previous publication [10]. The pipette solution contained (in mM): 140 NMDG chloride (NMDG-Cl), 2 $MgCl_2$, 5 $CaCl_2$, and 10 HEPES, pH 7.4 with NMDG. Cells were perfused with a bath solution containing (in mM): 145 NaCl, 5 KCl, 2 $MgCl_2$, 1 $CaCl_2$, 5 glucose, 5 HEPES, and 20 sucrose, pH 7.4 with NaOH. After the establishment of an inside-out configuration, the patch was perfused with a standard I/O solution (i.e., intracellular solution) containing (in mM): 150 NMDG-Cl, 2 $MgCl_2$, 10 EGTA, and 8 Tris, pH 7.4 with NMDG.

CFTR channel currents in inside-out patches were recorded at room temperature with an EPC-10 patch clamp amplifier, filtered at 100 Hz with an eight-pole Bessel filter (Warner Instrument Corp.) and captured onto a hard disk at a sampling frequency of 500 Hz. The membrane potential was held at −30 or -50 mV and the inward current was inverted for clear data presentation. CFTR was first activated by cytoplasmic application of 25 U ml^{-1} PKA catalytic subunit (Sigma) plus 2 mM ATP until the current reached the steady-state (~30 mins.) before changing the cytoplasmic solutions.

Data analysis and statistics

We used Igor-Pro (WaveMetrics) to measure steady-state mean currents (I_M) for macroscopic analyses. For microscopic analyses, recordings with less than 5 visible simultaneously-opening steps in the presence of potentiator were further filtered off-line at 50 Hz with a digital filter and used for single channel kinetic analysis using a program developed by Dr. Csanády [37, 50]. The resulting kinetic parameters, mean bursting time (τ_b) and interburst time (τ_{ib}), represent the

closing rate and the opening rate respectively. For the sake of convenience, investigators in the field have used τ_o and τ_c to represent these kinetic parameters [9, 10, 51]. Of note, because of the uncertainty in assigning the number of active channels in the patch, this method inevitably underestimates the number of functional channels in the patch, hence results in an overestimation of the P_o. Therefore, the reported P_o value for N1301K-CFTR should be considered as the maximal P_o.

ANOVA and Student's t test were performed for statistical analysis using Microsoft Excel. $p < 0.05$ was considered significant.

Reagents

Mg-ATP, PKA and 2'-deoxy ATP (2'-dATP) were purchased from Sigma (Saint Louis, MO, USA). N^6–(2-phenylethyl)-ATP (P-ATP) was purchased from Biolog Life Science Institute (Bremen, Germany). VX-770 and VX-661 were purchased from Selleck Chemicals (Houston, TX, USA). VX-809 was purchased from AOBIOUS INC (Gloucester, MA, USA). GLPG1837 was provided by Galapagos/AbbVie.

iii. Results

Pharmacological responses of N1303K to the CFTR potentiator GLPG1837

Moderate gating defects have been reported for the few N1303K channels that reach the cell membrane [20, 21]. Here, we used the CFTR potentiator GLPG1837 to quantify the gating defects associated with N1303K-CFTR. WT-CFTR data (Fig. 1A, C and D), reported in Yeh et al. (2017) [32], were presented

for comparison. Although 3 μM, a saturating concentration of GLPG1837 for WT-CFTR, increased ATP-induced currents of phosphorylated WT-CFTR by ~ 2-fold (Fig. 1A, D), the N1303K channels showed a lower sensitivity to GLPG1837 as seen in Fig. 1B: Increasing [GLPG1837] from 1 to 6 to 20 μM resulted in an incremental increase of the macroscopic N1303K-CFTR currents. A return of the macroscopic currents to the baseline level after application of the selective CFTR inhibitor $CFTR_{Inh-172}$ ensures that the macroscopic currents observed are from CFTR. Fold increase in macroscopic currents was calculated as the ratio of steady-state currents (I_M) with potentiator GLPG1837 to I_M without potentiator. In contrast to a maximal 2-fold increase of WT-CFTR current by GLPG1837, macroscopic N1303K-CFTR currents increase 16.8 ± 1.8 (n = 6) fold in the presence of 20.0 μM GLPG1837 (summarized in Fig. 1C). This ~17-fold increase of the macroscopic N1303K-CFTR currents sets an upper limit of P_O at 0.06 (1/17) in the absence of the potentiator.

The fold increase of the current increase by various concentrations of GLPG1837 was normalized to the effect at the saturating dose (20.0 μM), and subsequently fitted with the Hill equation yielding a $K_{1/2}$ of 0.9 μM (Fig. 1D; cf. 0.2 μM for WT-CFTR). Of note, our previous studies demonstrated a state-dependent binding of GLPG1837 on CFTR: open states bind GLPG1837 more tightly than closed states [32]. Thus, a rightward shift of the dose response relationship for the N1303K mutation is consistent with the idea that the P_o of N1303K-CFTR must be very low.

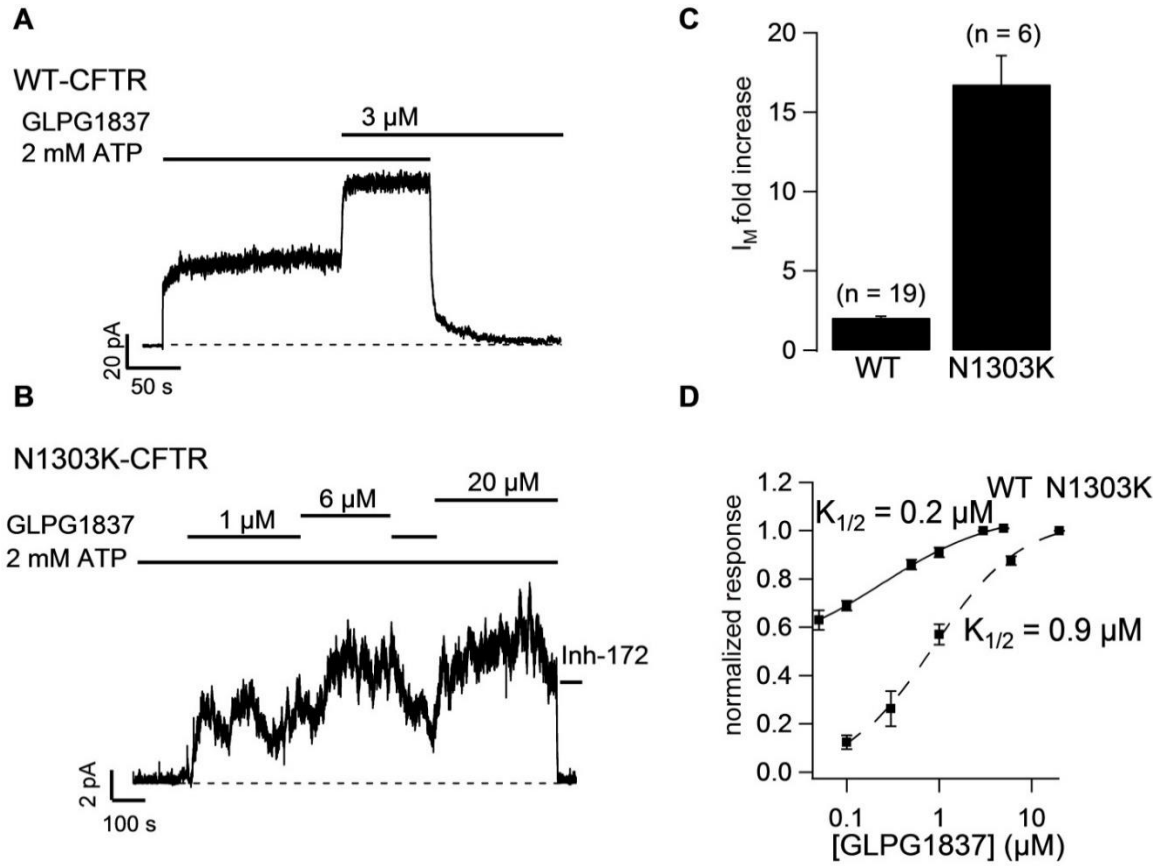

Figure 1. Macroscopic recordings of WT-CFTR (A) or N1303K-CFTR (B) showing response to potentiator GLPG1837. Channels were prephosphorylated with PKA + ATP and then exposed to GLPG1837. N1303K channel currents increase 16.8-fold ± 1.8 (n = 6) in response to a saturating concentration of GLPG1837, indicating a P_O for N1303K < 0.06. (C) Quantification of the fold increase in mean current (I_M) in response to saturating concentrations of GLPG1837. (D) GLPG1837 concentration response curves. The dose response curve is shifted to the right for N1303K-CFTR ($K_{1/2}$ = 0.9 μM cf. 0.2 μM for WT). Note data on WT-CFTR are extracted from ref. [32].

Microscopic gating kinetics of N1303K-CFTR

While the macroscopic analyses described above (Fig. 1) provide a reasonable estimation of the maximally possible P_O for N1303K channels in the absence of potentiator, kinetic analysis of microscopic current in patches containing fewer than 6 channels provides a much closer assessment of the

actual P_O for N1303K channels in the presence of potentiator. Figure 2A shows a representative recording of at least three N1303K-CFTR channels. In the absence of potentiator, only one opening event was seen in 30 seconds of the trace, making it virtually impossible to estimate the P_o. However, application of 20.0 μM GLPG1837 drastically increased channel activity thus increasing the probability of simultaneous channel opening events. This then allows us to more accurately estimate the number of functional channels in the patch. (Of note, although this method improves accuracy, the number of active channels may still be underestimated.) Kinetic analysis of data from such patches revealed a P_O of 0.44 ± 0.04 (n = 4) in the presence of 20.0 μM GLPG1837 and 2 mM ATP (Fig. 2B). We then back-calculated the P_O of N1303K channels in the absence of potentiator by dividing the P_O obtained in the presence of potentiator by the fold increase in mean current (I_M) by GLPG1837 (17-fold) to yield a P_O of ≤ 0.03 for N1303K-CFTR in the absence of potentiator. Interestingly, our analysis also revealed a paradoxical increase of the mean open time (τ_o) even without GLPG1837 (3.1 ± 0.8 s, n = 6; ~400 ms for WT-CFTR), consistent with previous reports of increased burst duration and decreased opening rate for N1303K [20]. The mean open time was further prolonged to 9.1 ± 3.1 s (n = 4) by GLPG1837 (vs. ~850 ms for WT-CFTR). Thus, the N1303K mutation causes a more severe gating defect than previously reported [20].

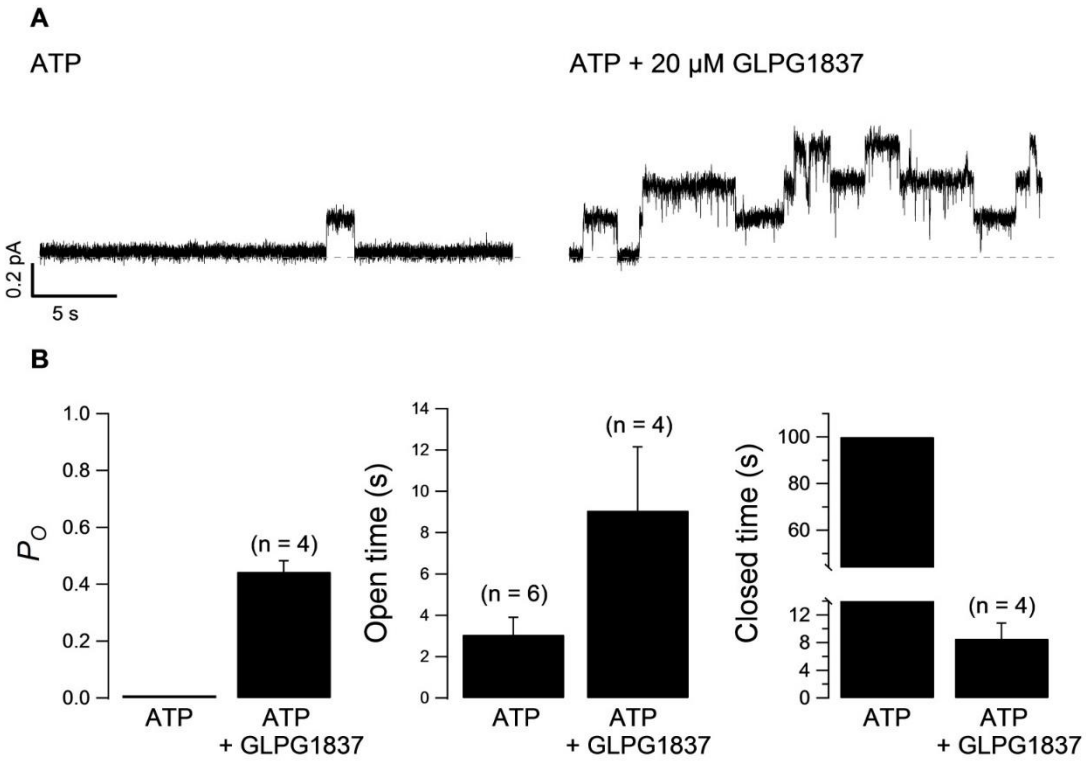

Figure 2. (A) Microscopic recording of N1303K-CFTR in ATP or ATP + GLPG1837. (B) Quantification of gating parameters P_O (B) mean open time (τ_O) (C) mean closed time (τ_O) (D) in the presence of ATP (P_O = 0.03; τ_O = 3.1 ± 0.8 s; τ_C = 100.0 sec) or ATP + GLPG1837 (P_O = 0.44 ± 0.04; τ_O = 9.1 ± 3.1 s; τ_C = 8.6 ± 2.2 s). Mean closed time in ATP was calculated based on $P_O = \tau_O/(\tau_O + \tau_C)$.

Response of N1303K-CFTR to ATP and ATP analogs

N1303 is located in CFTR's NBD2, which plays a critical role in controlling ATP-dependent opening and closing of the channel [43]. We therefore hypothesized that the gating defect associated with N1303K may be due to problems with how the mutant channel uses ATP as a ligand. We hence tested the N1303K mutant's response to ATP and to ATP analogs 2'-deoxy ATP (2'-dATP) and N^6-(2-phenylethyl)-ATP (P-ATP) in the continuous presence of GLPG1837. (Of note, the constant inclusion of GLPG1837 in the system ensures macroscopic currents that afford more accurate quantification.) In Fig. 3A, washout of ATP in the

presence of GLPG1837 resulted in a 35.5 ± 2.8% (n = 4) decrease in potentiated I_M, a result in stark contrast to the response of WT-CFTR channels to ATP removal shown in Fig. 1A. This observation indicates that N1303K channels do respond to ATP but the ATP dependence is much less than WT-CFTR. The hypothesis that the N1303K mutation results in an abnormal function of NBDs is further supported by the data shown in Fig. 3B and 3C. While it is known that d-ATP and P-ATP are more efficacious ligands than ATP for WT-CFTR gating [10, 52] exchanging ATP for d-ATP in the presence of GLPG1837 does not increase the currents of N1303K. More strikingly, replacing ATP with the high-affinity ATP analog P-ATP actually decreases the N1303K currents by 39.0 ± 7.0% (n = 4).

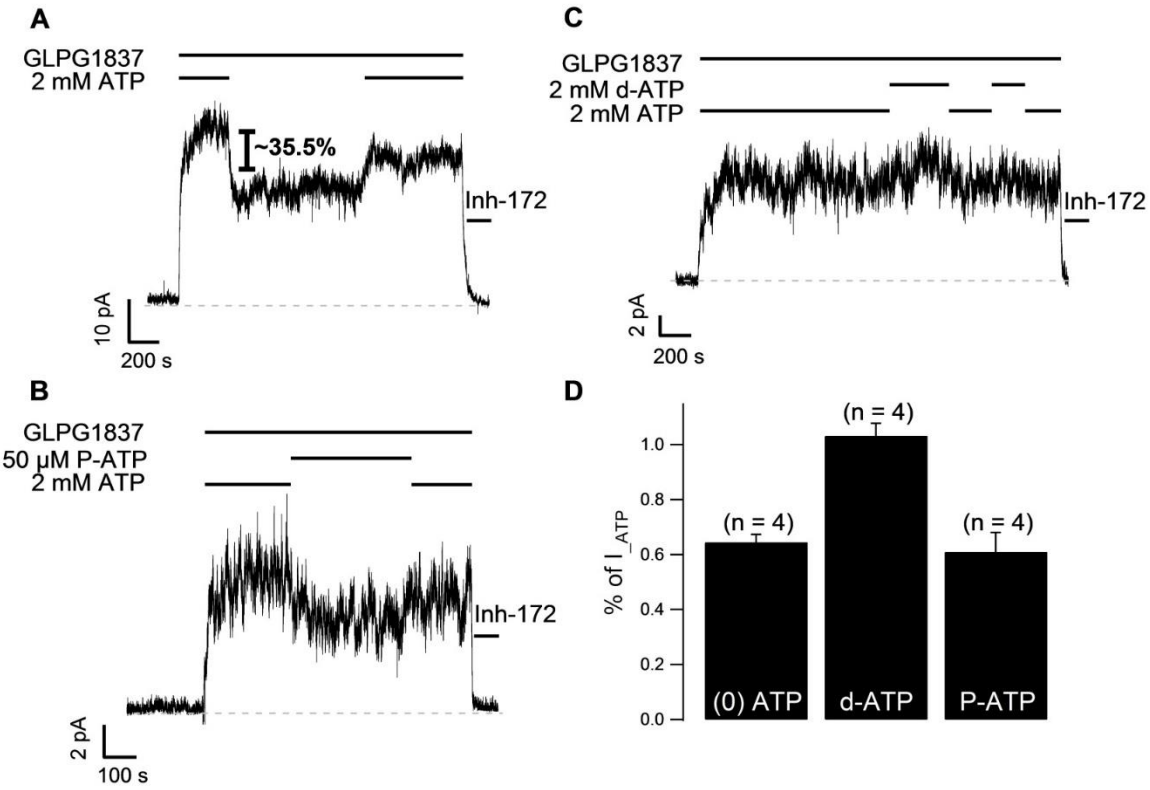

Figure 3. Macroscopic recordings of N1303K-CFTR showing its response to ATP (A) or ATP analogs P-ATP (B) or d-ATP (C) in the continuous presence of

GLPG1837. (D) Quantification of steady-state I_M in ATP-free solution, P-ATP or d-ATP presented as percent of I_M in ATP.

Pharmacological response of N1303K-CFTR to VX-770

We next tested if N1303K responds to VX-770, the only FDA approved CFTR potentiator for the treatment of patients with cystic fibrosis. A representative recording in Fig. 4A shows 200 nM VX-770 increased the P_O of N1303K channels. In Fig. 4B, the steady-state I_M in 500 nM VX-770 + ATP is about the same as the steady-state I_M in 200 nM VX-770, suggesting 200 nM is the maximally effective concentration of VX-770 for N1303K-CFTR. Using the maximally effective concentrations of GLPG1837 and VX-770, we compared the potentiators in the experimental protocol shown in Fig. 4C. Once the GLPG1837-potentiated N1303K currents reached a steady-state, the perfusion solution was switched to VX-770 + ATP. The steady-state I_M in GLPG1837 decreased about 50% upon switching to VX-770, indicating that GLPG1837 is ~2-fold more efficacious than VX-770.

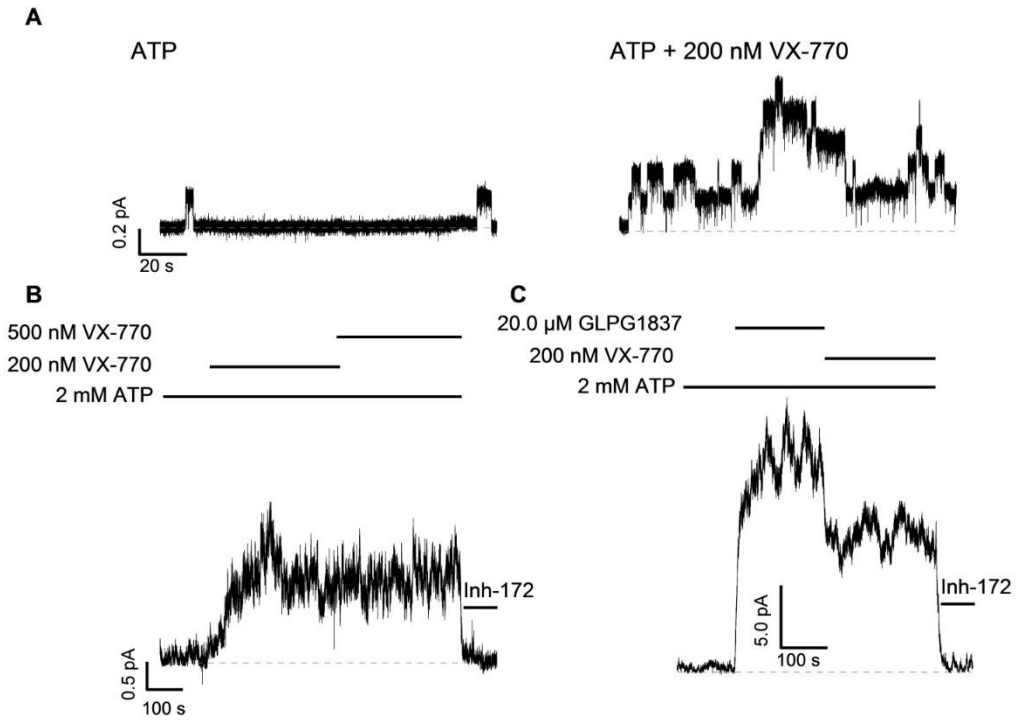

Figure 4. (A) Microscopic recording of N1303K-CFTR in ATP or ATP + VX-770. VX-770 can increase the P_O of N1303K channels. In (B), steady-state I_M potentiated with 200 nM VX-770 does not increase when the concentration of VX-770 is increased to 500 nM. (C) Macroscopic recording of N1303K-CFTR exposed first to GLPG1837 and then to VX-770. GLPG1837-potentiated I_M is reduced by 48.8 ± 4.8 % (n = 4), when the potentiator is switched to VX-770.

Defective biogenesis of N1303K is partly corrected with CFTR correctors VX-809, VX-661

N1303K is classified as a Class II mutation due to a decrease in Band C yield in Western blot analysis [17-19]. Consistent with these previous reports, we found N1303K has decreased surface expression compared to WT-CFTR. However, this trafficking defect caused by the N1303K mutation can be partly rectified by treatment of the cells with VX-809 (lane 2 in Fig. 5) or VX-661 (lane 5 in Fig. 5). Quantification of Band C yield normalized to vehicle-treated control shows VX-809 and VX-661 can increase the surface expression level by 2.86 ± 0.75 fold (n

= 10) and 2.94 ± 0.68 fold (n = 6) respectively. We next tested the effects of CFTR correctors in the presence of CFTR potentiators. Two CFTR potentiators, VX-770 and GLPG1837, were examined together with VX-809 or VX-661. Co-treatment with VX-770 or GLPG1837 did not counteract the effect of the correctors on the N1303K mutation (Fig. 5), in striking contrast to the reported effect of co-treatment with potentiator on pharmacologically corrected F508del [46, 47].

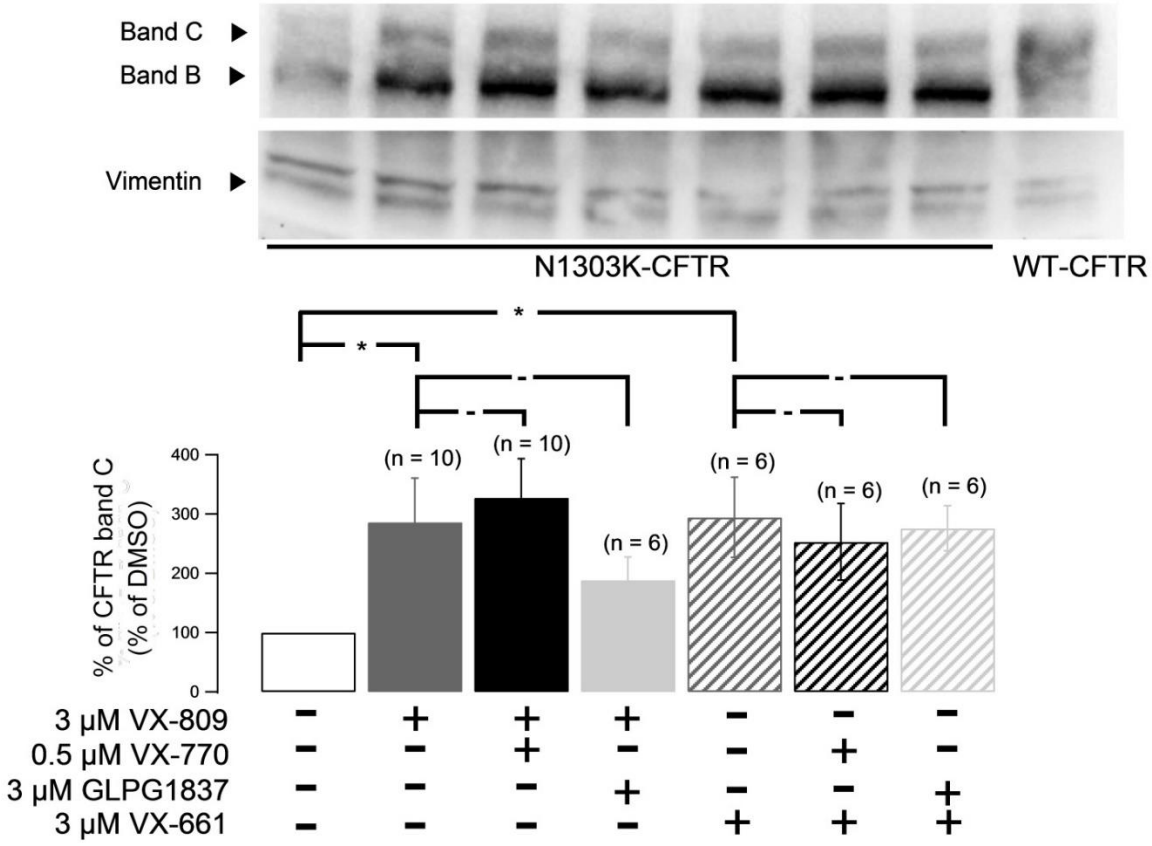

Figure 5. Western blot for N1303K-CFTR expressed in CHO cells. The cells were incubated for 18 h with DMSO, VX-809 (3 μM) or VX-661 (3 μM) alone and with GLGP1837 (3 μM) or VX-770 (0.5 μM) co-treatment. Assessing the amount of Vimentin using anti–Vimentin antibody served as loading control. The mature, complex glycosylated CFTR (Band C), and the immature, core glycosylated protein (Band B) are labeled. WT-CFTR is shown for comparison. Lower panel: Summary of Western blot results expressed as % increase of Band C yields

*normalized to vehicle (DMSO)-treated control. Error bars represent SEM. *, P < 0.05*

iv. Discussion

In this study, we have assessed the N1303K mutant's pharmacological response to CFTR modulators GLPG1837, VX-770, VX-809 and VX-661. Specifically, we have quantified the N1303K mutant's gating defects and shown a more severe defect than reported previously. The N1303K mutant's high constitutive activity in ATP-free solution and its abnormal response to ATP analogs P-ATP and d-ATP indicate the origin of its gating defects likely resides in CFTR's NBDs. We also provide evidence that GLPG1837 is a more efficacious but less potent potentiator of N1303K-CFTR than VX-770, as was previously reported for G551D-CFTR [32]. In this section, we will discuss the mechanism for the gating defects in N1303K-CFTR and clinical implications of our results.

N1303 and F508 are located at equivalent but opposite positions within the CFTR protein structure (Fig. S1A). F508 sits in the interface between NBD1 and the fourth intracellular loop (ICL4), aka the coupling helix of the CFTR's second transmembrane domains (TMD2) [4]. N1303, on the other hand, resides in the interface between NBD2 and ICL2 [4], and is thought to stabilize the Q-loop of NBD2 [53]. These two domain interfaces play important roles in CFTR gating because they serve to relay signals from the cytosolic NBDs to trigger conformational changes in the TMDs to open and close the gate [33, 34]. Not surprisingly, both F508del and N1303K mutations cause gating defects [20-22].

What is surprising however is that the two interface mutations show distinct gating patterns.

Despite >15-fold reduction in P_o mostly due to a lower opening rate, F508del retains ATP-dependence [15, 37, 38]. The function of F508del can be improved by maneuvers that promote NBD dimerization [15, 37] or abolish ATP hydrolysis [38]. It was proposed that F508del's low opening rate is due to a high enthalpy of the opening transition state reflecting strain at the NBD1-TMD interface [33]. Alternatively, ATP-binding induced dimerization of the NBDs in F508del is no longer tightly coupled to the opening of the gate in the TMDs. Although N1303K has about the same P_o as F508del, the gating function of N1303K is mostly irresponsive to the two ATP analogs tested. In addition, the prolonged open time of N1303K-CFTR is not altered by mutations that disrupt ATP hydrolysis or NBD dimerization (Fig. 7). This nearly complete uncoupling between NBDs and TMDs in N1303K-CFTR may result from a disruption of the Q-loop in NBD2, which plays a critical role in aligning the bound ATP at site 2 (composed of the head of NBD2 and the tail of NBD1) for catalyzing NBD dimerization [42]. Thus, despite the apparently opposite locations for F508 and N1303, mutations at these two positions result in similar but not identical dysfunction of the critical site 2 (see Fig. 6B & C for more detailed discussion).

Regardless of the mechanism underlying the gating defect caused by the N1303K mutation, our results bear important clinical implications. Here, we report that VX-770 increases the P_O of N1303K channels by ~ 8-fold. This, plus a ~3-fold improvement of N1303K biogenesis by either VX-809 or VX-661, and the

absence of negative drug-drug interaction with potentiator co-treatment suggest that a combination of corrector and potentiator may be a viable therapeutic option for patients bearing the N1303K allele. Indeed, a Phase II clinical trial with a combination of VX-661 (tezacaftor), a second generation corrector VX-440 and VX-770 (ivacaftor) reported favorable clinical outcomes for F508del heterozygotes carrying a minimal function mutation (e.g. N1303K) on their second allele.

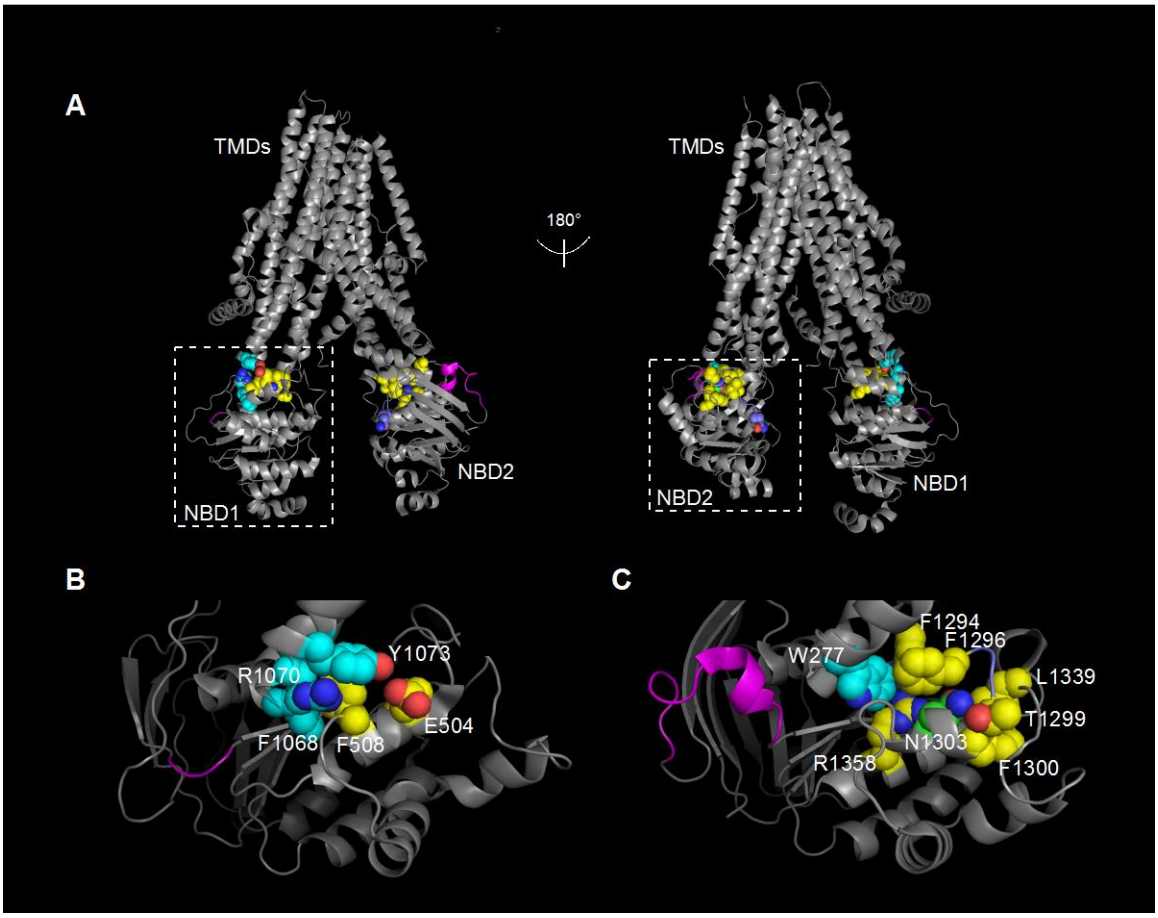

*Figure 6. (A) Cryo-EM structure of human CFTR in the unphosphorylated, ATP-free state adapted from Liu et al. (2016) [4]. TMDs: transmembrane domains; NBD1 and NBD2: first and second nucleotide binding domains respectively. Boxed regions are enlarged in panels **B** and **C**. (**B**) Expanded view of the NBD1-TMD2 interface highlighting F508 and E504 (in yellow) in NBD1, which contact*

*residues in ICL4 (F1068, R1070, Y1073 in cyan). Specifically, □□electron interactions may occur between F508 and R1070, and between F508 and F1068; the carboxyl side chain of E504 may form a hydrogen bond with the hydroxyl group in Y1073. In addition to these interface residues, F508 is also surrounded by W496 and M498 (not shown). (**C**) Expanded view of the NBD2-TMD1 interface showing the position of N1303 (in green), the side-chain of which does not contact ICL2, but instead interacts with the segment (in purple) leading to the conserved glutamine 1291 (not shown) of the so-called Q loop in NBD2. Specifically, N1303 is surrounded by intrinsic residues in NBD2 such as T1299, F1300, L1339, and R1358 (in yellow). The connection between NBD2 and ICL2 in this localized region is established by a cluster of aromatic amino acids including F1294, F1296 (in yellow) in NBD2 and W277 (in cyan) in ICL2. The side chain of N1303 may form hydrogen bonds with peptide backbone at positions F1296 and T1299 in the Q loop of NBD2; this latter interactions may explain why the N1303K mutation renders the gating motions in TMDs largely uncoupled to NBDs, as the Q1291 residue plays a critical role in aligning bound ATP in site 2 to catalyzing NBD dimerization. The N1303K mutation may also indirectly perturb the TMDs since the mutant channel exhibits stable open-channel conformation even in the absence of CFTR potentiator GLPG1837. In contrast, ATP-binding induced dimerization of the NBDs in F508del may be relatively intact, but NBD dimerization is no longer tightly coupled to the opening of the gate in the TMDs. This proposition is based on the expected loosening of NBD1-TMD2 interface when the contact between F508 and ICL4 is lost in F508del-CFTR. Note NBD1 lacks a β strand and an α helix (aka h2 in [35]) that are present in NBD2 (in magenta). Thus, unlike its counterpart TM4-ICL2-TM5 in the NBD2-TMD1 interface where this short α helix could serve as a doorstop that immobilizes the interface, when two NBDs coalesce to form a canonical dimer, TM10-ICL4-TM11 in TMD2 may have a higher probability to slip, especially in the case of F508del that weakens this interface contact. We therefore propose that although F508 and N1303 are located in a diagonal position in CFTR, F508del and N1303K mutations cause distinct gating defects by destroying the function of site 2 through different structural mechanisms. Images of cryo-EM structure of CFTR were prepared with PyMOL (version 1.3; Schrödinger) (PDB accession no. 5UAK).*

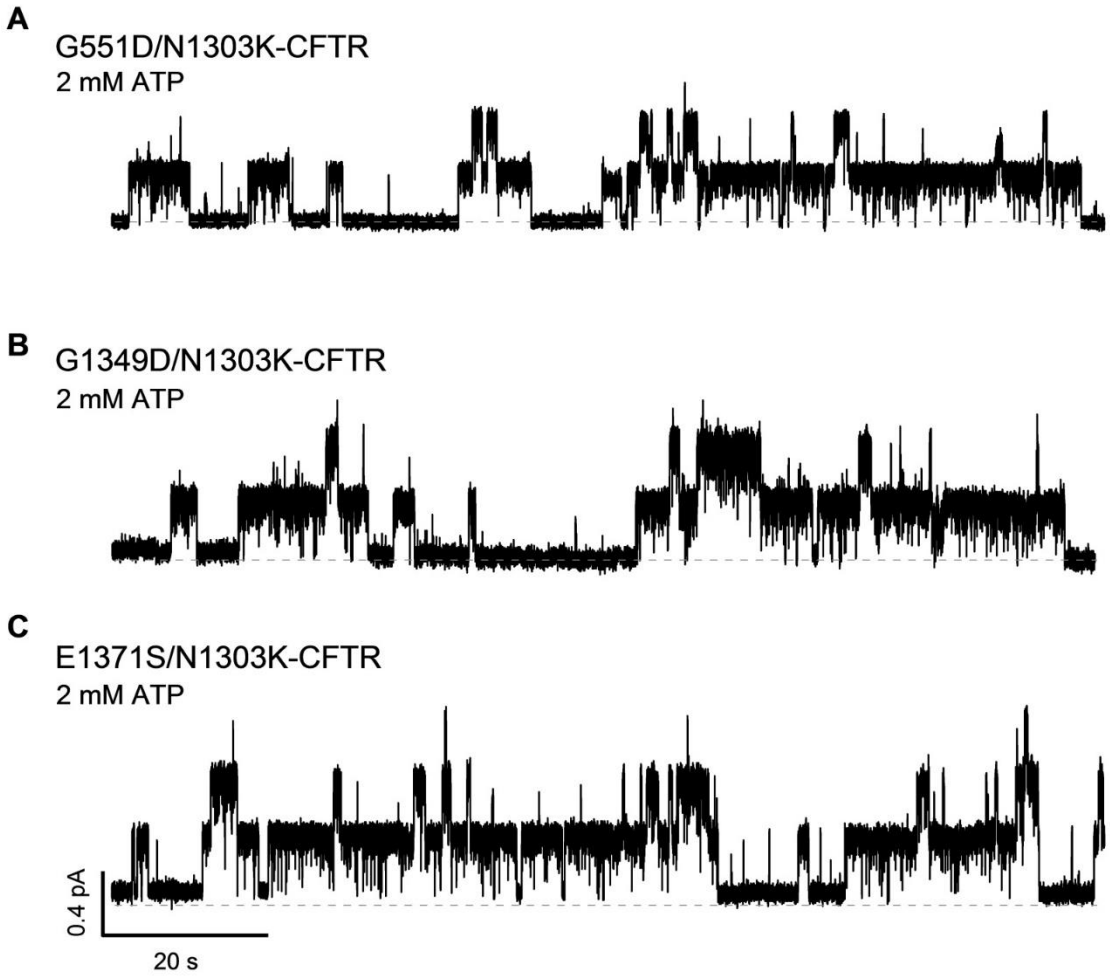

Figure 7. Representative single channel recordings of G551D/N1303K (A), G1349D/N1303K (B) and E1371S/N1303K at 2 mM ATP. Introducing a negatively charged aspartic acid into the signature sequence of ATP-binding site 1 (position 1349) or ATP-binding site 2 (position 551) may impede NBD dimerization via an electrostatic repulsion between the introduced negative charges and the bound ATP molecule. However, these second site mutations G551D (A) and G1349D (B) had no effect on N1303K mutant's long mean open time. Because the burst duration is determined by the rate of ATP hydrolysis in WT-CFTR, we introduced the E1371S mutation to the N1303K background (C). E1371S did not increase N1303K mutant's mean open time. Mean open times (τ_O) for G551D/N1303K, G1349D/N1303K and E1371S/N1303K are 3.0 ± 0.5 s (n = 3), 3.0 ± 1.1 s (n = 3) and 3.0 ± 0.3 s (n = 6), respectively. Note: τ_O = 3.1 ± 0.8 s for N1303K-CFTR (Fig. 2 in the text).

Chapter III: Future experiments

Future studies should aim to further elucidate the mechanism of N1303K gating dysfunction. Experiments 1-3 test the hypothesis N1303K mutation nearly completely uncouples the NBDs and TMDs, resulting from a disruption of the Q-loop in NBD2. Experiments 4-6 address an alternative hypothesis that NBD-TMD coupling remains at least partially intact in N1303K-CFTR.

1) N1303 is a conserved residue in many species including zebrafish. In zebrafish CFTR, the side chain of N1303 may be in closer contact with the peptide backbone of Q-loop residue 1296 in the closed, ATP-free state (PDB: 5UAR) than in the open, ATP-bound (PDB: 5W81) state. This interaction might provide evidence for N1303's role in an intra-NBD2 domain conformational change when ATP binds (site 2). In our study, all experiments were done using human CFTR. Recently, the full-length cryo-EM zebrafish CFTR structure has been resolved in both the ATP-free and ATP-bound states [35, 36]. These structures provide a convenient way to model hydrogen bonds within the Q loop. Therefore, we should assess N1303K gating defect in zebrafish CFTR.

2) N1303 participates in a hydrogen bond network with the NBD2 Q loop. Therefore, we can introduce mutations at site 1303, such as N1303Q, which may functionally mimic the hydrogen bond of N1303 with the peptide backbone of Q-loop residue 1296 in the ATP-free state but not ATP-bound state, to determine if restoring the hydrogen bond network can partially/completely rectify the gating defects. In support of this idea, mutations of N1303, such as N1303H, N1303I and N1303A, have similar kinetic effects to N1303K, and N1303H and N1303I

are disease-associated mutations [20]. These data may provide evidence that lose contact with the NBD2 Q loop is the molecular mechanism underlying N1303K gating defects.

3) N1303K mutation may indirectly perturb the TMDs since the mutant channel exhibits stable open-channel conformation even in the absence of CFTR potentiator GLPG1837. Therefore, we should test if mutations of Q loop residues F1294A and F1296A, which may contact the ICL2, exhibit phenotype similar to N1303K.

4) Although N1303K gating is severely defective, there are some opening events in the absence of potentiator. To determine whether N1303K retains O1 or O2 gating, we can continue experiments with N306D-N1303K or M348R-R352Q-N1303K (see [54] for details).

5) The N1303K gating defect is severe (P_O ≥ 16-fold less than WT-CFTR). Thus, even excised, inside-out patches containing hundreds of N1303K-CFTR channels yield only residual levels of current in the absence of potentiator. In this study, the fold increase in N1303K-mediated macroscopic currents in response to potentiator in excised, inside-out patches was calculated as the ratio of steady-state $I_{M\_potentiator}/I_{M\_ATP}$. In the future, whole cell experiments may be useful for a more accurate estimation of fold increase in I_M in response to potentiator.

6) In this study we have introduced mutations (G551D and G1349D) at the NBD dimer interface known to interfere with NBD dimerization (Fig. 7A & B). However, these second site mutations had no effect on N1303K mutant's long mean open

time. To fully assess the state of the NBDs in N1303K-CFTR, we can mutate the ATP-binding motifs in the head domains of NBD1 and NBD2. This maneuver is used to decrease ATP-binding affinity at the respective ATP-binding sites. N1303K resembles K1250A, a mutant which also has prolonged open time. However, in contrast to the reduced EC_{50} for ATP observed for mutations at K1250, the apparent EC_{50} for CFTR-N1303A (253 μM) is not different from that of wild type CFTR (176 μM) [20]. Therefore, while we have proposed a malfunction of ATP-binding site 2 for N1303K mutant, it may not be due to decreased ATP-binding affinity at ATP-binding site 2.

References

1. Gadsby DC, Nairn AC. Control of CFTR channel gating by phosphorylation and nucleotide hydrolysis. Physiological reviews. 1999;79(1 Suppl):S77-s107. Epub 1999/01/29. doi: 10.1152/physrev.1999.79.1.S77. PubMed PMID: 9922377.

2. Hwang TC, Kirk KL. The CFTR ion channel: gating, regulation, and anion permeation. Cold Spring Harbor perspectives in medicine. 2013;3(1):a009498. Epub 2013/01/04. doi: 10.1101/cshperspect.a009498. PubMed PMID: 23284076; PubMed Central PMCID: PMCPMC3530039.

3. Callebaut I, Eudes R, Mornon JP, Lehn P. Nucleotide-binding domains of human cystic fibrosis transmembrane conductance regulator: detailed sequence analysis and three-dimensional modeling of the heterodimer. Cellular and molecular life sciences : CMLS. 2004;61(2):230-42. Epub 2004/01/28. doi: 10.1007/s00018-003-3386-z. PubMed PMID: 14745501.

4. Liu F, Zhang Z, Csanady L, Gadsby DC, Chen J. Molecular Structure of the Human CFTR Ion Channel. Cell. 2017;169(1):85-95.e8. Epub 2017/03/25. doi: 10.1016/j.cell.2017.02.024. PubMed PMID: 28340353.

5. De la Rosa MB, Nelson SW. An interaction between the Walker A and D-loop motifs is critical to ATP hydrolysis and cooperativity in bacteriophage T4 Rad50. The Journal of biological chemistry. 2011;286(29):26258-66. Epub 2011/05/26. doi: 10.1074/jbc.M111.256305. PubMed PMID: 21610075; PubMed Central PMCID: PMCPMC3138309.

6. He L, Aleksandrov AA, Serohijos AW, Hegedus T, Aleksandrov LA, Cui L, et al. Multiple membrane-cytoplasmic domain contacts in the cystic fibrosis transmembrane conductance regulator (CFTR) mediate regulation of channel gating. The Journal of biological chemistry. 2008;283(39):26383-90. Epub 2008/07/29. doi: 10.1074/jbc.M803894200. PubMed PMID: 18658148; PubMed Central PMCID: PMCPMC2546535.

7. Sohma Y, and T.C. Hwang. 2015. Cystic Fibrosis and the CFTR Anion Channel. *In* Handbook of Ion Channels. CRC Press, Boca Raton, FL, 627-648. https://doi.org/10.1201/b18027-48.

8. Jih KY, Hwang TC. Nonequilibrium gating of CFTR on an equilibrium theme. Physiology (Bethesda, Md). 2012;27(6):351-61. Epub 2012/12/12. doi: 10.1152/physiol.00026.2012. PubMed PMID: 23223629; PubMed Central PMCID: PMCPMC4931552.

9. Jih KY, Hwang TC. Vx-770 potentiates CFTR function by promoting decoupling between the gating cycle and ATP hydrolysis cycle. Proceedings of

the National Academy of Sciences of the United States of America. 2013;110(11):4404-9. Epub 2013/02/27. doi: 10.1073/pnas.1215982110. PubMed PMID: 23440202; PubMed Central PMCID: PMCPMC3600496.

10. Tsai MF, Li M, Hwang TC. Stable ATP binding mediated by a partial NBD dimer of the CFTR chloride channel. The Journal of general physiology. 2010;135(5):399-414. Epub 2010/04/28. doi: 10.1085/jgp.201010399. PubMed PMID: 20421370; PubMed Central PMCID: PMCPMC2860585.

11. US CF Foundation JHU, The Hospital for Sick Children, The Clinical and Functional TRanslation of CFTR (CFTR2). http://cftr2.org. Accessed March 8, 2018.

12. Veit G, Avramescu RG, Chiang AN, Houck SA, Cai Z, Peters KW, et al. From CFTR biology toward combinatorial pharmacotherapy: expanded classification of cystic fibrosis mutations. Molecular biology of the cell. 2016;27(3):424-33. Epub 2016/01/30. doi: 10.1091/mbc.E14-04-0935. PubMed PMID: 26823392; PubMed Central PMCID: PMCPMC4751594.

13. Cheng SH, Gregory RJ, Marshall J, Paul S, Souza DW, White GA, et al. Defective intracellular transport and processing of CFTR is the molecular basis of most cystic fibrosis. Cell. 1990;63(4):827-34. Epub 1990/11/16. PubMed PMID: 1699669.

14. Dalemans W, Barbry P, Champigny G, Jallat S, Dott K, Dreyer D, et al. Altered chloride ion channel kinetics associated with the delta F508 cystic fibrosis mutation. Nature. 1991;354(6354):526-8. Epub 1991/12/19. doi: 10.1038/354526a0. PubMed PMID: 1722027.

15. Kopeikin Z, Yuksek Z, Yang HY, Bompadre SG. Combined effects of VX-770 and VX-809 on several functional abnormalities of F508del-CFTR channels. Journal of cystic fibrosis : official journal of the European Cystic Fibrosis Society. 2014;13(5):508-14. Epub 2014/05/07. doi: 10.1016/j.jcf.2014.04.003. PubMed PMID: 24796242.

16. Lukacs GL, Chang XB, Bear C, Kartner N, Mohamed A, Riordan JR, et al. The delta F508 mutation decreases the stability of cystic fibrosis transmembrane conductance regulator in the plasma membrane. Determination of functional half-lives on transfected cells. The Journal of biological chemistry. 1993;268(29):21592-8. Epub 1993/10/15. PubMed PMID: 7691813.

17. Gregory RJ, Rich DP, Cheng SH, Souza DW, Paul S, Manavalan P, et al. Maturation and function of cystic fibrosis transmembrane conductance regulator variants bearing mutations in putative nucleotide-binding domains 1 and 2. Molecular and cellular biology. 1991;11(8):3886-93. Epub 1991/08/01. PubMed PMID: 1712898; PubMed Central PMCID: PMCPMC361177.

18. Rapino D, Sabirzhanova I, Lopes-Pacheco M, Grover R, Guggino WB, Cebotaru L. Rescue of NBD2 mutants N1303K and S1235R of CFTR by small-molecule correctors and transcomplementation. PloS one. 2015;10(3):e0119796. Epub 2015/03/24. doi: 10.1371/journal.pone.0119796. PubMed PMID: 25799511; PubMed Central PMCID: PMCPMC4370480.

19. Dekkers JF, Gogorza Gondra RA, Kruisselbrink E, Vonk AM, Janssens HM, de Winter-de Groot KM, et al. Optimal correction of distinct CFTR folding mutants in rectal cystic fibrosis organoids. The European respiratory journal.

2016;48(2):451-8. Epub 2016/04/23. doi: 10.1183/13993003.01192-2015. PubMed PMID: 27103391.

20. Berger AL, Ikuma M, Hunt JF, Thomas PJ, Welsh MJ. Mutations that change the position of the putative gamma-phosphate linker in the nucleotide binding domains of CFTR alter channel gating. The Journal of biological chemistry. 2002;277(3):2125-31. Epub 2002/01/15. PubMed PMID: 11788611.

21. Randak C, Welsh MJ. An intrinsic adenylate kinase activity regulates gating of the ABC transporter CFTR. Cell. 2003;115(7):837-50. Epub 2003/12/31. PubMed PMID: 14697202.

22. Randak CO, Welsh MJ. ADP inhibits function of the ABC transporter cystic fibrosis transmembrane conductance regulator via its adenylate kinase activity. Proceedings of the National Academy of Sciences of the United States of America. 2005;102(6):2216-20. Epub 2005/02/03. doi: 10.1073/pnas.0409787102. PubMed PMID: 15684079; PubMed Central PMCID: PMCPMC548590.

23. http://www.cftr.info/about-cf/cftr-mutations/the-six-classes-of-cftr-defects/. [cited 2018 03-17].

24. Okiyoneda T, Veit G, Dekkers JF, Bagdany M, Soya N, Xu H, et al. Mechanism-based corrector combination restores DeltaF508-CFTR folding and function. Nature chemical biology. 2013;9(7):444-54. Epub 2013/05/15. doi: 10.1038/nchembio.1253. PubMed PMID: 23666117; PubMed Central PMCID: PMCPMC3840170.

25. Ren HY, Grove DE, De La Rosa O, Houck SA, Sopha P, Van Goor F, et al. VX-809 corrects folding defects in cystic fibrosis transmembrane conductance regulator protein through action on membrane-spanning domain 1. Molecular biology of the cell. 2013;24(19):3016-24. Epub 2013/08/09. doi: 10.1091/mbc.E13-05-0240. PubMed PMID: 23924900; PubMed Central PMCID: PMCPMC3784376.

26. Van Goor F, Hadida S, Grootenhuis PD, Burton B, Stack JH, Straley KS, et al. Correction of the F508del-CFTR protein processing defect in vitro by the investigational drug VX-809. Proceedings of the National Academy of Sciences of the United States of America. 2011;108(46):18843-8. Epub 2011/10/07. doi: 10.1073/pnas.1105787108. PubMed PMID: 21976485; PubMed Central PMCID: PMCPMC3219147.

27. Solomon GM, Marshall SG, Ramsey BW, Rowe SM. Breakthrough therapies: Cystic fibrosis (CF) potentiators and correctors. Pediatric pulmonology. 2015;50 Suppl 40:S3-s13. Epub 2015/06/23. doi: 10.1002/ppul.23240. PubMed PMID: 26097168; PubMed Central PMCID: PMCPMC4620567.

28. Van Goor F, Hadida S, Grootenhuis PD, Burton B, Cao D, Neuberger T, et al. Rescue of CF airway epithelial cell function in vitro by a CFTR potentiator, VX-770. Proceedings of the National Academy of Sciences of the United States of America. 2009;106(44):18825-30. Epub 2009/10/23. doi: 10.1073/pnas.0904709106. PubMed PMID: 19846789; PubMed Central PMCID: PMCPMC2773991.

29. Jih KY, Lin WY, Sohma Y, Hwang TC. CFTR potentiators: from bench to bedside. Current opinion in pharmacology. 2017;34:98-104. Epub 2017/10/27. doi: 10.1016/j.coph.2017.09.015. PubMed PMID: 29073476; PubMed Central PMCID: PMCPMC5723237.

30. Yu H, Burton B, Huang CJ, Worley J, Cao D, Johnson JP, Jr., et al. Ivacaftor potentiation of multiple CFTR channels with gating mutations. Journal of cystic fibrosis : official journal of the European Cystic Fibrosis Society. 2012;11(3):237-45. Epub 2012/02/02. doi: 10.1016/j.jcf.2011.12.005. PubMed PMID: 22293084.

31. Van Goor F, Yu H, Burton B, Hoffman BJ. Effect of ivacaftor on CFTR forms with missense mutations associated with defects in protein processing or function. Journal of cystic fibrosis : official journal of the European Cystic Fibrosis Society. 2014;13(1):29-36. Epub 2013/07/31. doi: 10.1016/j.jcf.2013.06.008. PubMed PMID: 23891399.

32. Yeh HI, Sohma Y, Conrath K, Hwang TC. A common mechanism for CFTR potentiators. The Journal of general physiology. 2017;149(12):1105-18. Epub 2017/10/29. doi: 10.1085/jgp.201711886. PubMed PMID: 29079713; PubMed Central PMCID: PMCPMC5715911.

33. Sorum B, Czege D, Csanady L. Timing of CFTR pore opening and structure of its transition state. Cell. 2015;163(3):724-33. Epub 2015/10/27. doi: 10.1016/j.cell.2015.09.052. PubMed PMID: 26496611.

34. Sorum B, Torocsik B, Csanady L. Asymmetry of movements in CFTR's two ATP sites during pore opening serves their distinct functions. eLife. 2017;6.

Epub 2017/09/26. doi: 10.7554/eLife.29013. PubMed PMID: 28944753; PubMed Central PMCID: PMCPMC5626490.

35. Zhang Z, Chen J. Atomic Structure of the Cystic Fibrosis Transmembrane Conductance Regulator. Cell. 2016;167(6):1586-97.e9. Epub 2016/12/03. doi: 10.1016/j.cell.2016.11.014. PubMed PMID: 27912062.

36. Zhang Z, Liu F, Chen J. Conformational Changes of CFTR upon Phosphorylation and ATP Binding. Cell. 2017;170(3):483-91.e8. Epub 2017/07/25. doi: 10.1016/j.cell.2017.06.041. PubMed PMID: 28735752.

37. Miki H, Zhou Z, Li M, Hwang TC, Bompadre SG. Potentiation of disease-associated cystic fibrosis transmembrane conductance regulator mutants by hydrolyzable ATP analogs. The Journal of biological chemistry. 2010;285(26):19967-75. doi: 10.1074/jbc.M109.092684. PubMed PMID: 20406820; PubMed Central PMCID: PMCPMC2888408.

38. Jih KY, Li M, Hwang TC, Bompadre SG. The most common cystic fibrosis-associated mutation destabilizes the dimeric state of the nucleotide-binding domains of CFTR. The Journal of physiology. 2011;589(Pt 11):2719-31. Epub 2011/04/14. doi: 10.1113/jphysiol.2010.202861. PubMed PMID: 21486785; PubMed Central PMCID: PMCPMC3112550.

39. Hopfner KP, Karcher A, Craig L, Woo TT, Carney JP, Tainer JA. Structural biochemistry and interaction architecture of the DNA double-strand break repair Mre11 nuclease and Rad50-ATPase. Cell. 2001;105(4):473-85. Epub 2001/05/24. PubMed PMID: 11371344.

40. Smith PC, Karpowich N, Millen L, Moody JE, Rosen J, Thomas PJ, et al. ATP binding to the motor domain from an ABC transporter drives formation of a nucleotide sandwich dimer. Molecular cell. 2002;10(1):139-49. Epub 2002/08/02. PubMed PMID: 12150914; PubMed Central PMCID: PMCPMC3516284.

41. Chen J, Lu G, Lin J, Davidson AL, Quiocho FA. A tweezers-like motion of the ATP-binding cassette dimer in an ABC transport cycle. Molecular cell. 2003;12(3):651-61. Epub 2003/10/07. PubMed PMID: 14527411.

42. Higgins CF, Linton KJ. The ATP switch model for ABC transporters. Nature structural & molecular biology. 2004;11(10):918-26. Epub 2004/09/29. doi: 10.1038/nsmb836. PubMed PMID: 15452563.

43. Hwang TC, Yeh JT, Zhang J, Yu YC, Yeh HI, Destefano S. Structural mechanisms of CFTR function and dysfunction. The Journal of general physiology. 2018. Epub 2018/03/28. doi: 10.1085/jgp.201711946. PubMed PMID: 29581173.

44. Riordan JR, Rommens JM, Kerem B, Alon N, Rozmahel R, Grzelczak Z, et al. Identification of the cystic fibrosis gene: cloning and characterization of complementary DNA. Science (New York, NY). 1989;245(4922):1066-73. Epub 1989/09/08. PubMed PMID: 2475911.

45. Wainwright CE, Elborn JS, Ramsey BW, Marigowda G, Huang X, Cipolli M, et al. Lumacaftor-Ivacaftor in Patients with Cystic Fibrosis Homozygous for Phe508del CFTR. The New England journal of medicine. 2015;373(3):220-31. Epub 2015/05/20. doi: 10.1056/NEJMoa1409547. PubMed PMID: 25981758; PubMed Central PMCID: PMCPMC4764353.

46. Cholon DM, Quinney NL, Fulcher ML, Esther CR, Jr., Das J, Dokholyan NV, et al. Potentiator ivacaftor abrogates pharmacological correction of DeltaF508 CFTR in cystic fibrosis. Science translational medicine. 2014;6(246):246ra96. Epub 2014/08/08. doi: 10.1126/scitranslmed.3008680. PubMed PMID: 25101886; PubMed Central PMCID: PMCPMC4272825.

47. Veit G, Avramescu RG, Perdomo D, Phuan PW, Bagdany M, Apaja PM, et al. Some gating potentiators, including VX-770, diminish DeltaF508-CFTR functional expression. Science translational medicine. 2014;6(246):246ra97. Epub 2014/08/08. doi: 10.1126/scitranslmed.3008889. PubMed PMID: 25101887; PubMed Central PMCID: PMCPMC4467693.

48. Bompadre SG, Li M, Hwang TC. Mechanism of G551D-CFTR (cystic fibrosis transmembrane conductance regulator) potentiation by a high affinity ATP analog. The Journal of biological chemistry. 2008;283(9):5364-9. Epub 2008/01/03. doi: 10.1074/jbc.M709417200. PubMed PMID: 18167357.

49. Lin WY, Jih KY, Hwang TC. A single amino acid substitution in CFTR converts ATP to an inhibitory ligand. The Journal of general physiology. 2014;144(4):311-20. Epub 2014/09/17. doi: 10.1085/jgp.201411247. PubMed PMID: 25225552; PubMed Central PMCID: PMCPMC4178940.

50. Csanady L. Rapid kinetic analysis of multichannel records by a simultaneous fit to all dwell-time histograms. Biophys J. 2000;78(2):785-99. doi: 10.1016/S0006-3495(00)76636-7. PubMed PMID: 10653791; PubMed Central PMCID: PMCPMC1300681.

51. Vergani P, Lockless SW, Nairn AC, Gadsby DC. CFTR channel opening by ATP-driven tight dimerization of its nucleotide-binding domains. Nature. 2005;433(7028):876-80. doi: 10.1038/nature03313. PubMed PMID: 15729345; PubMed Central PMCID: PMCPMC2756053.

52. Aleksandrov AA, Aleksandrov L, Riordan JR. Nucleoside triphosphate pentose ring impact on CFTR gating and hydrolysis. FEBS letters. 2002;518(1-3):183-8. Epub 2002/05/09. PubMed PMID: 11997043.

53. Eudes R, Lehn P, Ferec C, Mornon JP, Callebaut I. Nucleotide binding domains of human CFTR: a structural classification of critical residues and disease-causing mutations. Cellular and molecular life sciences : CMLS. 2005;62(18):2112-23. Epub 2005/09/01. doi: 10.1007/s00018-005-5224-y. PubMed PMID: 16132229.

54. Zhang J, Hwang TC. Electrostatic tuning of the pre- and post-hydrolytic open states in CFTR. The Journal of general physiology. 2017;149(3):355-72. Epub 2017/03/01. doi: 10.1085/jgp.201611664. PubMed PMID: 28242630; PubMed Central PMCID: PMCPMC5339510.